

University of Texas Rio Grande Valley

ScholarWorks @ UTRGV

---

Chemistry Faculty Publications and Presentations

College of Sciences

---

1-2015

## Imaging, Spectroscopy, Mechanical, Alignment and Biocompatibility Studies of Electrospun Medical Grade Polyurethane (Carbothane™ 3575A) Nanofibers and Composite Nanofibers Containing Multiwalled Carbon Nanotubes

Faheem A. Sheikh

*The University of Texas Rio Grande Valley*

Javier Macossay-Torres

*The University of Texas Rio Grande Valley*

Travis Cantu

*The University of Texas Rio Grande Valley*

Xujun Zhang

*The University of Texas Rio Grande Valley*

M. Shamshi Hassan

Follow this and additional works at: [https://scholarworks.utrgv.edu/chem\\_fac](https://scholarworks.utrgv.edu/chem_fac)

See next page for additional authors

 Part of the [Chemistry Commons](#), and the [Nanoscience and Nanotechnology Commons](#)

---

### Recommended Citation

Macossay, J., Sheikh, F. A., Cantu, T., Eubanks, T. M., Salinas, M. E., Farhangi, C. S., Ahmad, H., Hassan, M. S., Khil, M., Maffi, S. K., Kim, H., & Bowlin, G. I. (2014). Imaging, spectroscopic, mechanical and biocompatibility studies of electrospun Tecoflex® EG 80A nanofibers and composites thereof containing multiwalled carbon nanotubes. *Applied Surface Science*, 321, 205–213. <https://doi.org/10.1016/j.apsusc.2014.09.198>

This Article is brought to you for free and open access by the College of Sciences at ScholarWorks @ UTRGV. It has been accepted for inclusion in Chemistry Faculty Publications and Presentations by an authorized administrator of ScholarWorks @ UTRGV. For more information, please contact [justin.white@utrgv.edu](mailto:justin.white@utrgv.edu), [william.flores01@utrgv.edu](mailto:william.flores01@utrgv.edu).

---

**Authors**

Faheem A. Sheikh, Javier Macossay-Torres, Travis Cantu, Xujun Zhang, M. Shamshi Hassan, M. Esther Salinas, Chakavak S. Farhangi, Hassan Ahmad, Hern Kim, and Gary L. Bowlin

Published in final edited form as:

*J Mech Behav Biomed Mater.* 2015 January ; 41: 189–198. doi:10.1016/j.jmbbm.2014.10.012.

## Imaging, Spectroscopy, Mechanical, Alignment and Biocompatibility Studies of Electrospun Medical Grade Polyurethane (Carbothane™ 3575A) Nanofibers and Composite Nanofibers Containing Multiwalled Carbon Nanotubes

Faheem A. Sheikh<sup>a,b,\*</sup>, Javier Macossay<sup>a,\*</sup>, Travis Cantu<sup>a</sup>, Xujun Zhang<sup>a</sup>, M. Shamshi Hassan<sup>c</sup>, M. Esther Salinas<sup>a</sup>, Chakavak S. Farhangi<sup>a</sup>, Hassan Ahmad<sup>a</sup>, Hern Kim<sup>d</sup>, and Gary L. Bowlin<sup>e</sup>

<sup>a</sup>Department of Chemistry, University of Texas-Pan American, Edinburg, TX 78539, USA

<sup>b</sup>Nano-Bio Regenerative Medical Institute, College of Medicine, Hallym University, Chuncheon, 200-702, South Korea

<sup>c</sup>Department of Organic Materials and Fiber Engineering, Chonbuk National University, Jeonju 561-756, South Korea

<sup>d</sup>Energy and Environment Fusion Technology Center, Department of Energy and Biotechnology, Myongji University, Yongin, Kyonggi-do 449-728, Republic of Korea

<sup>e</sup>Department of Biomedical Engineering, The University of Memphis, Memphis, TN 38152, USA

### Abstract

In the present study, we discuss the electrospinning of medical grade polyurethane (Carbothane™ 3575A) nanofibers containing multi-walled-carbon-nanotubes (MWCNTs). A simple method that does not depend on additional foreign chemicals has been employed to disperse MWCNTs through high intensity sonication. Typically, a polymer solution consisting of polymer/MWCNTs has been electrospun to form nanofibers. Physicochemical aspects of prepared nanofibers were evaluated by SEM, TEM, FT-IR and Raman spectroscopy, confirming nanofibers containing MWCNTs. The biocompatibility and cell attachment of the produced nanofiber mats were investigated while culturing them in the presence of NIH 3T3 fibroblasts. The results from these tests indicated non-toxic behavior of the prepared nanofiber mats and had a significant attachment of cells towards nanofibers. The incorporation of MWCNTs into polymeric nanofibers led to an improvement in tensile stress from  $11.40 \pm 0.9$  to  $51.25 \pm 5.5$  MPa. Furthermore, complete alignment of the nanofibers resulted in an enhancement on tensile stress to  $72.78 \pm 5.5$  MPa. Displaying these attributes of high mechanical properties and non-toxic nature of nanofibers are recommended for an ideal candidate for future tendon and ligament grafts.

© 2014 Elsevier Ltd. All rights reserved.

\*Corresponding authors: Faheem A Sheikh, Ph.D. ph: +82-10-7264-0315, fax: +82-33-251-0503: faheem99in@yahoo.com. Javier Macossay, Ph.D. ph: +956-665-3377 fax: +956-665-5006: jmacossay@utpa.edu.

**Publisher's Disclaimer:** This is a PDF file of an unedited manuscript that has been accepted for publication. As a service to our customers we are providing this early version of the manuscript. The manuscript will undergo copyediting, typesetting, and review of the resulting proof before it is published in its final citable form. Please note that during the production process errors may be discovered which could affect the content, and all legal disclaimers that apply to the journal pertain.

## Keywords

Electrospinning; Nanofibers; Dispersion; Cytotoxicity; Mechanical properties

---

## Introduction

It is regarded that a decrease in size of any material into the nano-scale can dramatically increase the surface area, surface roughness and surface area-to-volume ratios, which can ultimately lead to superior physiochemical properties of materials. The production of nano-sized fibers by the electrospinning technique was documented by a series of patents by (Formhals and Richard, 1934; Formhals 1939, 1940, 1943 and 1944). After these pioneering works, there has been an exponential growth of this technique in different medical and non-medical fields (Huang et al., 2003). During the electrospinning process, a high voltage power supply is used to create an electrically charged jet or melt into a Taylor cone, which further on, evaporates to leave a polymer fiber collected on the opposite electrode (Sheikh et al., 2011, 2012). In the past two decades, the electrospinning technique has been attracting a tremendous attention due to a resultant web-like matrix that mimics the topology of the extracellular matrix (ECM) present in the human body, and these matrices can be used as scaffold in tissue-engineering applications (Bhattacharai et al., 2004).

Modification in electrospinning parameters and apparatus generates fibers with a desirable nanoscale size, which have been studied in controlled drug release, gene delivery, tissue engineering, wound healing and other applications (Yu et al., 2009; Zhang et al., 2011; Pham et al., 2006). These nanofibers with desirable properties have been extensively investigated in biomedical applications, in particular for tissue engineering aspects (Bhattacharai et al., 2004). However, electrospun fibers are typically collected in a random manner which limits their applications, both in mechanical and in cell spreading. Therefore, there have been attempts to align nanofibers so as to grow cells in a guided tissue regeneration (GTR) manner (Corey et al., 2007; Meng et al., 2010). It has been reported that preparing nanofibers with aligned orientation not only helps cells to grow faster, but also improves the mechanical properties of the electrospun mats (Moffat et al., 2009).

Multi-walled-carbon-nanotubes (MWCNTs) are considered to be unique materials due to their excellent mechanical, electrical and thermal conductivity along with the high chemical stability. These unique promising properties of MWCNTs has permitted their use in a broad range of applications (Ma et al., 2010). Recently, it had been noticed that poly(lactic-co-glycolic acid) (PLGA) nanofibers incubated using simulated body fluid can impart gradient mineralization and futuristically help in repair of tendons (Lipner et al., 2014). Fabrication of random and aligned nanoyarn-reinforced nanofibers based on silk fibroin and poly(l-lactide-co-caprolactone) indicated nanoyarn enforced nanofibers have high mechanical properties which promisingly suggests its favorable attribute towards manufacture of artificial tendon (Yang et al., 2014). With this impression, cell-free and cell-laden fibers are reviewed, revealing an introduction of carbon nanotubes can remarkably influence the mechanical properties of nanofibers (Tamayol et al., 2013). It was observed that, tensile strength of (0.66 and 0.85 MPa) can be obtained from calcium alginate and chitosan-alginate

composite nanofibers (Lee, B.R et al., 2011; Lee, G.-S et al., 2011). Moreover, poly( $\epsilon$ -caprolactone) (PCL) nanofibers with 0.5% of MWCNTs possessed maximum tensile strength of 1.42 MPa (Meng et al., 2010). Furthermore, biodegradable poly-DL-lactide (PLA) nanofibers with 3% of MWCNTs showed maximum Young's modulus of (77.8 to 91.3 MPa), for random and aligned nanofiber composites (Shao et al., 2011). The most attractive attribute of MWCNTs is to use these nano-sized fillers as reinforcing materials into a polymer matrix, and then use them as a biomaterial where high tensile stresses and loads are needed. By introducing small amounts of MWCNTs into a polymer nanofiber, the mechanical requirements for artificial tendon and ligament prostheses can be addressed. In this direction, there are various reports that deal with the improvement in existing mechanical properties of nanofibers through the use of MWCNTs (Meng et al., 2010; Shao et al., 2011; Xiao et al., 2010; Xuyen et al., 2009). Further, the degree of dispersion and alignment of MWCNTs in the polymer matrix, which finally results in proper re-enforcement is an important issue (Ma et al., 2010). Generally, a stable and uniform suspension of nanotubes in the polymer is required to obtain a fine dispersion in the final product, which can be achieved using chemical modification or by the use of surfactants. However, these approaches introduce defects and/or residual surfactants can be in detrimental to material in terms of toxicity to final product (biomaterials). A perfect strategy to introduce MWCNTs in the nanofibers which have a ECM mimicking factor with reliable mechanical properties are having a promising potential in substitution of soft and hard tissues; including vasculature, bone, neural, tendon and/or ligament (Sill and von Recum, 2008).

In this report, we demonstrate the preparation of Carbothane™ 3575A nanofibers with MWCNTs embedded within the polymer matrix, without the use of additional chemicals. The obtained nanofibers were characterized by various spectroscopic techniques to determine the interactions between the polymer matrix and the MWCNTs. The cell cytotoxicity, towards NIH 3T3 fibroblast indicated that the nanofibers were non-toxic, while the addition of MWCNTs and nanofiber alignment resulted in an improvement on their mechanical properties.

## Materials and methods

The MWCNTs used in this study were obtained from Bayer Materials and used as received. According to the manufacturer specifications, the MWCNTs (Baytubes®C 150 HP) present an outer diameter of ~13 nm, inner diameter of ~4 nm and length of ~1  $\mu$ m. Medical grade polyurethane Carbothane™ 3575A was kindly supplied by Lubrizol Advanced Materials. Tetrahydrofuran (THF, 99%) and N, N-dimethylformamide (DMF, 99.8%) were purchased from Sigma-Aldrich, (USA), and used without further purification. NIH 3T3 mouse fibroblast cells were purchased from ATCC, Manassas, VA. Dulbecco's Modified Eagle Medium supplemented with 10% newborn calf serum and Antibiotic-Antimycotic 100x were purchased from Gibco® and Invitrogen™. 0.4% Trypan blue was acquired from Invitrogen™, MTT reagent and DMSO 99.9% were acquired from Sigma-Aldrich, (USA), and 0.25% Trypsin-EDTA for cell harvest from Gibco® and Invitrogen™. Glycine was purchased from BioRad Laboratories to form glycine buffer, which was prepared by taking 0.1M glycine in 0.1M NaCl, followed by equilibration with 0.1N NaOH to pH=10.5.

Treated tissue culture flasks and microplates for cell growth and seeding were purchased from Fisher Scientific, (USA).

### 1.1. Preparation of polymeric solutions for electrospinning

A 15 wt% solution of Carbothane™ 3575A was prepared by dissolving the polymer pellets in THF and DMF. Initially, pellets were dissolved overnight in THF, and then DMF was added to give the final concentration that contained 15 wt% of polymer in THF:DMF (1:1, v/v). In the case of preparing solutions containing MWCNTs, a stepwise methodology was adopted. In the first phase, MWCNTs in DMF were agitated by using an ultra-high sonicating device. This was achieved by using (Sonics Vibra-cell model VCX 500) operating at 20 kHz with an amplitude of 20%. The ultra-sonic agitation was allowed to continue for a period of 1 h in the presence of an ice-bath, so as to keep the solution free from excessive heat generated due to sonication. Thereafter, samples were viewed as homogeneously dispersed and well stable with a dark ink-like appearance without being precipitated for several months. Further on, the dispersed MWCNTs in DMF were added to the previously dissolved Carbothane™ 3575A solutions in THF, to have final mixtures containing 0.06%, 0.33% and 0.66% of MWCNTs.

### 1.2. Electrospinning process

Polymeric solutions used for electrospinning were injected by using a 10 mL glass syringe with a 22 needle gauge (0.7 mm OD × 0.4 mm ID) at a flow rate of 0.01 mL/min, which was controlled using a KDS 210 pump (KD Scientific Holliston, Inc., MA). High power supply equipment (ES30P-5W and ES30N-5W for positive and negative voltages, respectively) was used to eject out the nanofibers from the needle tip; these apparatus were purchased from Gamma High Voltage Research (Ormond Beach, FL). The copper wire originating from the positive electrode (anode) with an applied voltage of +17 kV was connected to the needle tip through an alligator clip, and a negative electrode (cathode) with an applied voltage of -17 kV was attached to the round metallic collector. The solutions were electrospun with a 15 cm working distance (the distance between the needle tip and the collector). The as-spun nanofibers were dried under vacuum for 24 h in the presence of P<sub>2</sub>O<sub>5</sub> to remove the residual moisture. For aligning nanofibers, three different rotation speeds of the collector drum were adjusted to produce randomly-obtained, semi-aligned and completely aligned nanofibrous morphologies (Meng et al., 2010). To obtain these different morphologies, the rotation speeds of the collector were set at 798, 3240 and 5740 rpm, respectively.

### 1.3. Cell culture studies

To study cell cytotoxicity of the obtained nanofibers, fibroblasts were cultured from a frozen ampoule and were allowed to propagate into a 25 cm<sup>2</sup> culture flask in DMEM, supplemented with 10% newborn calf serum and 1% Antibiotic-Antimycotic 100x in a humidified incubator with 5% CO<sub>2</sub> environment at 37°C temperature. After achieving 70–80% of confluent growth, the cell population was carefully sub-cultured to reach 25,000 cell/mL, cells were counted using a Countess® automated cell counter. For cell seeding on nanofibers surfaces, 160 µl of DMEM containing 25,000 cell/mL were added to experimental microplate wells and allowed to grow for 24h, to create a favorable environment before the nanofibers were introduced. After 24h of incubation of initial cell

seeding, the media was taken out and 80 $\mu$ L of fresh media was added into the wells. At this point, the samples punched out (6 mm in diameter) nanofibers (which were previously sterilized by exposure of Ethanol and UV light to eliminate contaminants) were added to the 96 well microplates and 80  $\mu$ L of fresh media was added to each experimental well in order to have a final volume of 160  $\mu$ L. Finally, the microplates were incubated at 37°C with 5% of CO<sub>2</sub> for a period of (3, 5 and 7 days), during the incubation time exhausted media was replenished at the 3 day mark.

#### 1.4. Cell viability test by MTT assay

The MTT assay was performed to check the cell viability after culturing the NIH 3T3 fibroblasts in the presence of pristine nanofibers and nanofibers modified with MWCNTs for a period of (3, 5 and 7 days). The assay monitors the production of reducing mitochondrial cell enzymes, which can react with MTT salts to form noted purple color formazan dye, giving absorbance under UV spectrophotometer. This reaction only occurs when reductase enzymes are active therefore, the conversion of one color to another is used as a measure of living cells. In order to use this useful tool for cell viability, after the desired days of incubation, MTT reagent (5mg/mL) in PBS was prepared, from which a 40  $\mu$ L aliquot was added to each well of microplates and left to incubate for four hours. During the incubation period, cells undergo the aforementioned reaction, producing a purple color product which can be quantified spectrophotometrically using a (microplate reader Bio-rad model 680). After the 4h incubation period, the contents from 96-wells were taken in a separate centrifuge tube and centrifuged at 3500 rpm. Existing media was completely aspirated and 160  $\mu$ L of DMSO was added followed by 20  $\mu$ L of glycine buffer; and the plate was kept on a shaker for 5 minutes to allow these solutions to mix properly. Prior to obtaining readings, all nanofibers were carefully removed from each well and the contents of the wells were determined on a microplate reader at a wavelength of 595 nm using DMSO/glycine buffer as control.

### Characterization

A scanning electron microscope (SEM) EVO<sup>®</sup> LS10 (Carl Zeiss SMT., Ltd) was used to investigate the morphology of the nanofibers. The samples were coated by using a thin layer of silver-palladium for a 180 sec for two consecutive cycles at 45mA with the (Desk II Denton Vacuum Cold Sputter) prior to imaging. Then, micrographs from each sample were taken at an accelerating voltage of 10.75 KV. Transmission electron microscopy (TEM) JEOL JEM 2010 operating at 200 kV, JEOL Ltd., Japan was used to investigate the presence and location of the MWCNTs embedded within nanofibers. The samples for investigation were obtained by placing the TEM 300-mesh copper grid close to the tip of the syringe needle for a few seconds during the electrospinning process, followed by vacuum-drying and finally observed under TEM. The thermal stability of the nanofiber mats was carried out with a TGA 7 (Perkin Elmer Co., USA) by heating from 30°C to 700°C at a rate of 10°C/min under a continuous nitrogen purge, having a flow rate of 20 mL/min. The study of functional groups in polymer structure and its interactions with the MWCNTs was investigated through Fourier-Transform Infrared (FTIR) analysis. The spectra were recorded by grinding fiber samples with KBr to subsequently form pellets, which were analyzed using

a Bruker (IFS 55) from 4000-700  $\text{cm}^{-1}$  with a 4  $\text{cm}^{-1}$  resolution and 32 scans. Raman spectra for samples were obtained at 785 nm laser excitation on a Bruker Optics Raman Spectrometer (BX51). The laser power density was kept as 10 mW with 50 integrations, having 2 co-additions and  $25 \times 100$  nm of aperture. Spectra were collected from at least from 4 different locations, using a microscope with 50X magnification; obtained data was averaged to plot final graphs. The mechanical properties of the nanofiber mats was investigated by using INSTRON<sup>®</sup> tensile tester 5943, with a 25 N maximum load cell under a crosshead speed of 10 mm/min. Samples were cut in the form of a 'dog-bone' shaped via die cutting from nonwoven mats with (2.75 mm wide at their narrowest point with a gage length of 7.5 mm). At least six specimens were tested for tensile behavior and the average values were reported. In order to facilitate the visualization of cell attachment pattern and cell survival on the surfaces of nanofibers, chemical fixation of cells was carried out for each sample after 7 days of incubation in presence of NIH 3T3 fibroblasts. Nanofiber samples in 96-well plates were rinsed twice with phosphate buffer saline (PBS) and subsequently fixed in 2.5 vol. % glutaraldehyde for 1h. After cell fixation, samples were rinsed with PBS and then serially de-hydrated with graded concentration of ethanol, (i.e., 20%, 30%, 50%, 70% and 100% vol. ethanol) for 10 min each. To remove the residual ethanol, the samples were kept in a vacuum oven for 12 hrs and then observed under SEM. Samples were coated and observed under the same conditions as described previously.

## Results and discussions

Electrospinning of polymeric solutions containing various amounts of MWCNTs resulted in fabrication of defect free and bead-free morphologies (Figure 1). As presented in (Fig. 1a), it can be observed that electrospinning of pure Carbothane<sup>™</sup> 3575A solutions resulted in smooth, uniform, continuous and bead-free nanofibers. Moreover, the morphology of nanofibers containing MWCNTs are represented in (Fig. 1b, c and d), providing evidence that the nanofibrous morphology was not affected by the addition of MWCNTs. However, it can be observed that there is a reasonable decrease in fiber diameters due to the addition of MWCNTs. For this reason, the average nanofiber diameters were calculated from randomly selected individual fibers (15–20 individual diameters measured per sample) using (Adobe Photoshop 6.0). Figure 2 presents the bar graphs for the average nanofiber diameters. The pristine nanofibers had an average diameter of  $714 \pm 196$  nm, and the nanofibers modified with 0.06%, 0.33% and 0.66% of MWCNTs had diameters of  $570 \pm 149$  nm,  $370 \pm 196$  nm and  $361 \pm 96$  nm, respectively. From these results, it can be concluded that a sharp decrease in diameters occurred with the incorporation of MWCNTs. These results are in complete agreement with the previously reported cases where high charge densities of the polymer jet leads to an increase on the stretching of the polymer droplet, which overall helps to decrease the fiber diameter (Barakat et al., 2009). In our case, the effect is attributed to the presence of highly conductive MWCNTs in the polymeric solution, reducing the diameters of the nanofibers during electrospinning (Barakat et al., 2009).

The porosity of nanofibers used for tissue engineering is an important consideration to be taken care for efficient cell proliferation. High porosity can help to have frequent flow of nutrients to the cells growing in scaffolds and can have an enhanced cell anchoring to the pores which can results in plugging of pores after the cells attain the maximum growth. In



this connection, the average diameter of nanofibers was calculated from SEM images (30 individual pore diameters measured per sample) using (Adobe Photoshop 6.0), and it was observed that addition of MWCNTs do favorably improve the porosity of nanofibers. For instance, pristine nanofibers had least average pore diameters of  $136 \pm 66$  nm. Comparatively, for nanofibers with 0.06%, 0.33% and 0.66% of MWCNTs had average larger pore diameters of  $148 \pm 82$  nm,  $990 \pm 483$  nm and  $1151 \pm 561$  nm, respectively, which is higher than the pristine counterpart. Moreover, same trend was followed with the large pore diameter calculation. For instance, for pristine nanofibers large pore diameter was calculated to be 320 nm. And, for the nanofibers with 0.06%, 0.33% and 0.66% of MWCNTs had higher large pore diameters of 341 nm, 2534 nm and 2455 nm, respectively. Furthermore, small pore diameter also showed the same trend for pristine nanofibers of 40 nm of small pore diameters, and nanofibers modified with 0.06%, 0.33% and 0.66% of MWCNTs with larger small pore diameters of 41 nm, 344 nm and 411 nm, respectively. Overall, these results indicate that addition of MWCNTs do influence in increasing porosity of nanofibers.

To investigate the presence and location of MWCNTs within the nanofibers, TEM was utilized. In this regard, Figures 3a and b show the micrographs of the nanofibers with MWCNTs, in their low and high magnifications. From these images, a clear presence of MWCNTs alongside the nanofiber direction can be observed. Arrows indicated in these figures show that MWCNTs are well-dispersed and aligned along the nanofiber direction. Furthermore, the high magnification image (Fig. 3b) from the encircled area shows that the MWCNTs are perfectly unbundled due to the sonication process followed.

Figure 4 represents the FT-IR spectra of nanofibers. The spectra show minute shifts in the functional groups due to the addition of MWCNTs. It can be observed that peaks in pristine nanofibers appeared at ( $2934\text{ cm}^{-1}$  and  $2848\text{ cm}^{-1}$ ), which are due to asymmetric or symmetric stretching in (C-H) in  $\text{CH}_2$ . In the fingerprint region of the polymer (i.e.,  $1745\text{ cm}^{-1}$  to  $957\text{ cm}^{-1}$ ), we can see the peak at  $1745\text{ cm}^{-1}$ , which is due to the stretching mode of (C=O) of the urethane amide I. The peak at  $1529\text{ cm}^{-1}$  appears due to the stretching mode in (C-N) and (N-H) of the amide II band. The peaks at  $1452\text{ cm}^{-1}$  and  $1403\text{ cm}^{-1}$  are due to bending vibrations in  $\text{CH}_2$  groups. Also, the peak positioned at  $956\text{ cm}^{-1}$  is attributed to the in-plane  $\text{CH}_2$  bending vibration in  $\text{CH}_2$  groups (Yang et al., 1999). The peaks at  $1745\text{ cm}^{-1}$ ,  $1529\text{ cm}^{-1}$ ,  $1452\text{ cm}^{-1}$  and  $1403\text{ cm}^{-1}$  in the case of nanofibers containing MWCNTs exhibited shifts towards higher frequencies, indicating the interaction between the polymer chains and the MWCNTs. These shifts are indicative of proper dispersion and non-specific covalent interaction between the  $\sigma$  bond in C-N and the  $\pi$  electrons from MWCNTs (Chipara et al., 2013).

It is well know that MWCNTs do have a high thermal stability, therefore do have high on-set degradation temperatures. Accordingly, it was believed that incorporation of MWCNTs will enhance the thermal stability of nanofibers, which can indirectly be co-related with appropriate dispersion of MWCNTs among the nanofibers. Also, nanofibers modified with MWCNTs will possess an increased on-set temperature than that of pristine nanofibers. To prove this hypothesis and highlight the proper dispersion of MWCNTs among the nanofibers (Figure 5) presents the TGA results of the obtained nanofiber. It is observed that

the pristine nanofibers have on-set decomposition temperature at 296°C, while the nanofibers containing the MWCNTs showed higher on-sets temperatures of 310°C, 312°C and 319°C, respectively. This increase confirmed the incorporation of MWCNTs, and demonstrated the expected higher thermal stability of nanofibers modified with MWCNTs when proper dispersion is achieved.

Figure 6 presents the Raman spectra of pure polymer nanofibers, MWCNTs, and the nanofibers modified with MWCNTs. In case of pristine nanofibers, the small peaks existing in the spectra situated at 1441  $\text{cm}^{-1}$ , 1304  $\text{cm}^{-1}$ , 1105  $\text{cm}^{-1}$ , 1066  $\text{cm}^{-1}$  and 1036  $\text{cm}^{-1}$  are due to different stretching and vibrational modes from various functional groups present in the pure polymeric nanofibers. This figure also presents the spectra of pure MWCNTs, and it indicates that mainly two peaks located at the position of 1600  $\text{cm}^{-1}$  and 1306  $\text{cm}^{-1}$ . Basically, there are mainly two vibrational modes observed for Raman scattering in MWNTs, one is the tangential G-band vibrations which falls within range of (1550  $\text{cm}^{-1}$  to 1605  $\text{cm}^{-1}$ ) and another vibration mode is due to disordered-induced by D-band at ~1350  $\text{cm}^{-1}$  (Zheng and Xu, 2010). Accordingly, it can be observed that pure MWCNTs possess the peaks at the position of 1600  $\text{cm}^{-1}$  and 1306  $\text{cm}^{-1}$  accounting for the vibration modes in the G and D bands which is similar to that of mentioned in references (Liu et al., 2006). The spectra of modified nanofibers with MWCNTs, shows that the vibrations induced by the tangential G-band can be located at 1607  $\text{cm}^{-1}$ , 1607  $\text{cm}^{-1}$  and 1609  $\text{cm}^{-1}$  for 0.06%, 0.33% and 0.66% of MWCNTs in nanofibers, respectively. The D-band can be located at 1308  $\text{cm}^{-1}$ , 1310  $\text{cm}^{-1}$  and 1315  $\text{cm}^{-1}$  in nanofibers with 0.06%, 0.33% and 0.66% of MWCNTs (Zheng and Xu, 2010; Liu et al., 2006). It is observed that up-shifts in the tangential G-band and in the D-band occur when MWCNTs are added to the system, and that higher concentrations enhance the effect. In fact, the strong attachment of the polymer to nanotubes resulting due to hydrophobic and vander Waals attractions between the polymer and the graphite sheet increases the energy required for vibrations to occur, which is reflected in the higher frequencies observed (Yadav et al., 2011).

Figure 7 shows the data originated from the MTT assay after 1, 3 and 7 days of culturing NIH 3T3 fibroblasts. In this figure, we can clearly observe the growth in cell control, which follow the same trend as that of pristine and nanofibers containing MWCNTs. These observations indicate that fibroblasts cultured in the presence of pristine nanofibers and/or nanofibers modified with MWCNTs are normally growing indicating non-toxic in nature of used materials. It can also be observed that the growth proceeds in an exponential manner. Furthermore, Figure 8 shows the pattern of fibroblast attachment on nanofibers. The cells were cultured for 7 days, and then fixed on the nanofibers as described in (Section 2). From this data, it is evident that the cells are perfectly attached onto the nanofibers surface with clearly observable cytoplasmic extensions. Moreover, the high magnification images from the encircled area provide more insight about the pattern of growth on the nanofiber surfaces. This confluent growth shown by all combinations of nanofibers coincides with the results from the MTT assay in Figure 7. Overall, these results confirm the non-toxic behavior of these nanofibers towards the NIH 3T3 fibroblasts.

The results from the stress vs. strain curves on nanofibers (Fig. S2 and S3), indicated that there is a gradual increase on the mechanical properties of the nanofibers as MWCNTs were

added, except for the maximum loading. The average tensile stress from these curves was  $11.40 \pm 0.9$  MPa for pristine nanofibers, and the nanofibers with MWCNTs (0.06%, 0.33% and 0.66%) presented average tensile stress of ( $39.60 \pm 1.4$ ,  $51.25 \pm 5.5$ , and  $32.99 \pm 0.8$  MPa), respectively. These values are remarkably higher than the PCL-nanofibers modified with 0.5% MWCNTs, which had an average tensile stress of 1.42 MPa, and PCL reinforced collagen nanofibers had higher tensile stress of 77.8 to 91.3 MPa (Meng et al., 2010; Bialorucki et al., 2014). It can be seen that in the case of 0.06% and 0.33% addition of MWCNTs, a significant improvement in stress was obtained, than the pristine one; however, this property was decreased by further addition of MWCNTs. This decrease, which is the case for nanofibers containing 0.66% of MWCNTs (i.e., higher concentration), can be accounted due to improper dispersion of MWCNTs (Meng et al., 2010). It is well known that nano-materials have high surface energy and re-aggregate easily, which can lead to the poor dispersion. A good dispersion of MWCNTs in a polymer matrix is needed for more uniform stress distribution, which will increase the interfacial area for stress transfer from the polymer matrix to the MWCNTs (Moniruzzaman et al., 2007). Also, it is possible that the inadequate sonication conditions at the highest MWCNTs concentration can keep them in bundled state, which results in a non-uniform dispersion within the nanofibers.

As aforementioned, GTR is gaining much attention because of the preference of growing cells in a particular direction which results in filling the gap between damaged tissues at faster rates (Corey et al., 2007; Meng et al., 2010). It has been suggested that aligned nanofibers can tolerate much stress than the nanofibers with random morphologies, therefore giving improved mechanical strength (Corey et al., 2007; Meng et al., 2010). With this intention, we designed nanofibers containing 0.33% MWCNTs (i.e., combination with highest mechanical properties) with different alignments, which were obtained by varying the rotation speeds of the collector (798, 3240 and 5740 rpm). The resultant nanofiber membranes were named as random, semi-aligned and completely aligned. The nanofiber combination with 0.33% of MWCNTs was ideally selected as represented the highest stress bearing capacity of ( $51.25 \pm 5.5$  MPa). The SEM results for morphology of nanofibers after using three different speeds of collecting drum is presented in Figure 9. This Figure shows the random morphology of the nanofibers with MWCNTs at 798 rpm (Fig. 9a), at 3240 rpm with a semi-aligned structure (Fig. 9b), and at 5740 rpm with a completely aligned nanofiber structure (Fig. 9c). Moreover, the in-set figure in Figure 9c shows the high magnification of the completely aligned nanofibers. From these figures, we can observe that as the rotation-speed of the collector increases, the nanofiber morphology transforms from random to semi-aligned and further to completely aligned nanofibers. From (Fig. 9c), which shows the nanofibers with completely aligned morphology, further enriches the justification (TEM results Fig. 3), that MWCNTs can be uniformly packed along the nanofiber direction.

Moreover, results from mechanical properties of these three nanofibers combination indicated that the average stress with random, semi-aligned and completely-aligned nanofibers was  $51.25 \pm 5$ ,  $51.15 \pm 8$ , and  $72.78 \pm 5$  MPa, respectively (Figs. S4 and S5). In case PLA nanofibers, modified with 3% of MWCNTs showed maximum Young's modulus of (77.8 and 91.3 MPa), for random and aligned nanofiber composites (Shao et al., 2011). We believe the reason could be proper dispersion caused of MWCNTs and due to high solubility PLA, compared to dissolving Carbothane™ 3575A in DMF and THF solvents.

Moreover, the obvious increase in the obtained tensile stress for the obtained nanofibers in this study while aligning them suggests the use of these nanofibers in artificial tendon and ligament prostheses, where high mechanical properties are a prerequisite. Furthermore, a complete cell culture study, with aligned and non-aligned nanofibers is ongoing and will be reported in future publications.

## Conclusion

In conclusion, the artificial ligaments and tendons should represent excellent mechanical performance comparable to that of naturally existing one and biocompatibility are the primary requirements for these materials before considering for tissue engineering application. In this connection, fabrication of nanofibers incorporating MWCNTs was achieved, and these nanofibers present enhanced tensile stress and good mechanical properties. A simple method using high intensity sonication for MWCNTs in DMF was effective in de-bundling nanotubes at low concentrations, and the introduction of the MWCNTs in the polymeric solution led to a decrease in the diameter of nanofibers. Furthermore, addition of MWCNTs resulted in increased mechanical properties of the nanofibers and increase in porosity. TEM was used to investigate the presence and location of MWCNTs in the nanofibers, while FTIR revealed the functional groups interacting with the MWCNTs. Raman spectroscopy confirmed the interaction between the nano-fillers and the polymeric matrix, also indicating that the sonication process afforded de-bundled MWCNTs. The cell culture study indicated the non-toxicity of the produced nanofibers, and suggests their potential use in biomedical applications. Finally, an additional enhancement to the nanofiber construct containing 0.33% MWCNTs, which yielded highest mechanical property was obtained through alignment by changing the collector speed, suggesting the role of aligned nanofibers with advanced mechanical properties in construction of artificial tendon and ligaments.

## Supplementary Material

Refer to Web version on PubMed Central for supplementary material.

## Acknowledgments

This work was financially supported by the National Institutes of Health grant # 1SC2AG036825-01, for which JM is gratefully acknowledged. The authors wish to acknowledge Mr. Joseph D. Ventura from Bayer Materials Science for providing the Multiwalled Carbon Nanotubes used in these studies and Mr. Raul Salazar from Lubrizol Advanced Materials for providing Carbothane™ 3575A. Faheem A Sheikh and Hern Kim do acknowledge the support by National Research Foundation of Korea (NRF)–Grants funded by the Ministry of Science, ICT and Future Planning (2012K1A3A1A30055020) and the Ministry of Education (2009-0093816), Republic of Korea.

## References

- Barakat NAM, Kanjwal MA, Sheikh FA, Kim HY. Spider-net within the N6, PVA and PU electrospun nanofiber mats using salt addition: Novel strategy in the electrospinning process. *Polymer*. 2009; 50:4389–4396.10.1016/j.polymer.2009.07.005
- Bhattarai SR, Bhattarai N, Yi HK, Hwang PH, Cha DI, Kim HY. Novel biodegradable electrospun membrane: scaffold for tissue engineering. *Biomaterials*. 2004; 25:2595–2602.10.1016/j.biomaterials.2003.09.043 [PubMed: 14751745]

- Bialorucki C, Subramanian G, Elsaadany M, Yildirim-Ayan E. In situ osteoblast mineralization mediates post-injection mechanical properties of osteoconductive material. *J Mech Behav Biomed Mater.* 2014; 38:143–153.10.1016/j.jmbbm.2014.06.018 [PubMed: 25051152]
- Chipara DM, Macossay J, Ybarra AVR, Chipara AC, Eubanks TM, Chipara M. Raman spectroscopy of polystyrene nanofibers-Multiwalled carbon nanotubes composites. *Appl Surf Sci.* 2013; 275:23–27.10.1016/j.apsusc.2013.01.116
- Corey JM, Lin DY, Mycek KB, Chen Q, Samuel S, Feldman EL, Martin DC. Aligned electrospun nanofibers specify the direction of dorsal root ganglia neurite growth. *J Biomed Mater Res Part A.* 2007; 83:636–645.10.1002/jbm.a.31285
- Formhals A, Richard SG. Process and apparatus for preparing artificial threads. US Patent. 1934; 1:975, 504.
- Formhals A. Method of Producing Artificial Fiber. US Patent. 1939; 2:158, 415.
- Formhals A. Artificial Thread and Method of Producing Same. US Patent. 1940; 2:187, 306.
- Formhals A. Production of artificial fibers from fiber forming liquids. US Patent. 1943; 2:323.025.
- Formhals A. Method and apparatus for spinning. US Patent. 1944; 2:349, 950.
- Huang ZM, Zhang YZ, Kotaki M, Ramakrishna S. A review on polymer nanofibers by electrospinning and their applications in nanocomposites. *Compos Sci Technol.* 2003; 63:2223–2253.10.1016/S0266-3538(03)00178-7
- Lee BR, Lee KH, Kang E, Kim DS, Lee SH. Microfluidic wet spinning of chitosan-alginate microfibers and encapsulation of HepG2 cells in fibers. *Biomicrofluidics.* 2011; 5:022208, p1–9.10.1063/1.3576903
- Lee GS, Park JH, Shin US, Kim HW. Direct deposited porous scaffolds of calcium phosphate cement with alginate for drug delivery and bone tissue engineering. *Acta Biomaterialia.* 2011; 7:3178–3186.10.1016/j.actbio.2011.04.008 [PubMed: 21539944]
- Lipner J, Liu W, Liu Y, Boyle J, Genin GM, Xia Y, Thomopoulos S. The mechanics of PLGA nanofiber scaffolds with biomimetic gradients in mineral for tendon-to-bone repair. *J Mech Behav Biomed Mater.* 2014; 40:59–68.10.1016/j.jmbbm.2014.08.002 [PubMed: 25194525]
- Liu A, Honma I, Ichihara M, Zhou H. Poly(acrylic acid)-wrapped multi-walled carbon nanotubes composite solubilization in water: definitive spectroscopic properties. *Nanotechnology.* 2006; 17:2845–2849.10.1088/0957-4484/17/12/003
- Ma PC, Siddiqui NA, Marom G, Kim JK. Dispersion and functionalization of carbon nanotubes for polymer-based. *Composites: Part A.* 2010; 41:1345–1367.10.1016/j.compositesa.2010.07.003
- Meng ZX, Wang YS, Maa C, Zheng W, Li L, Zheng YF. Electrospinning of PLGA/gelatin randomly-oriented and aligned nanofibers as potential scaffold in tissue engineering. *Mater Sci Eng, C.* 2010; 30:1204–1210.10.1016/j.msec.2010.06.018
- Meng ZX, Zheng W, Li L, Zheng YF. Fabrication and characterization of three-dimensional nanofiber membrane of PCL-MWCNTs by electrospinning. *Mater Sci Eng, C.* 2010; 30:1014–1021.10.1016/j.msec.2010.05.003
- Moffat KL, Anne MS, Kwei SP, Spalazzi JP, Doty SB, Levine WN, Lu HH. Novel Nanofiber-Based Scaffold for Rotator Cuff Repair and Augmentation. *Tissue Eng Part A.* 2009; 15:115–126.10.1089/ten.tea.2008.0014 [PubMed: 18788982]
- Moniruzzaman M, Chattopadhyay J, Billups WE, Winey KI. Tuning the Mechanical Properties of SWNT/Nylon 6, 10 Composites with Flexible Spacers at the Interface. *NanoLett.* 2007; 7:1178–1185.10.1021/nl062868e
- Pham QP, Sharma U, Mikos AG. Electrospinning of Polymeric Nanofibers for Tissue Engineering Applications: A Review. *Tissue Eng.* 2006; 12:1197–1211.10.1089/ten.2006.12.1197 [PubMed: 16771634]
- Shao S, Zhou S, Li L, Li J, Luo C, Wang J, Li X, Weng J. Osteoblast function on electrically conductive electrospun PLA/MWCNTs nanofibers. *Biomaterials.* 2011; 32:2821–2833.10.1016/j.biomaterials.2011.01.051 [PubMed: 21292320]
- Sheikh FA, Cantu T, Macossay J, Kim H. Fabrication of Polyvinylidene (PVDF) nanofibers containing nickel nanoparticles as future energy server materials. *Sci Adv Mater.* 2011; 3:216–222. <http://dx.doi.org/10.1166/sam.2011.1148>.

- Sheikh FA, Kanjwal MA, Macossay J, Barakat NAM, Kim HY. A simple approach for synthesis, characterization and bioactivity of bovine bones to fabricate the polyurethane nanofiber containing hydroxyapatite nanoparticles. *eXPRESS Polym Lett.* 2012; 6:41–53.10.3144/expresspolymlett.2012.5
- Sill TJ, von Recum HA. Electrospinning: applications in drug delivery and tissue engineering. *Biomaterials.* 2008; 29:1989–2006.10.1016/j.biomaterials.2008.01.011 [PubMed: 18281090]
- Tamayol A, Akbari M, Annabi N, Paul A, Khademhosseini A, Juncker D. Fiber-Based Tissue Engineering: Progress, Challenges, and Opportunities. *Biotechnol Adv.* 2013; 31:669–687.10.1016/j.biotechadv.2012.11.007 [PubMed: 23195284]
- Xiao S, Shen M, Guo R, Huang Q, Wang S, Shi X. Fabrication of multiwalled carbon nanotube-reinforced electrospun polymer nanofibers containing zero-valent iron nanoparticles for environmental applications. *J Mater Chem.* 2010; 20:5700–5708.10.1039/C0JM00368A
- Xuyen NT, Kim TH, Geng H-Z, Lee IH, Kim KK, Lee YH. Three-dimensional architecture of carbon nanotube-anchored polymer nanofiber composite. *J Mater Chem.* 2009; 19:7822–7825.10.1039/B913762A
- Yadav SK, Mahapatra SS, Yoo HJ, Cho JW. Synthesis of multi-walled carbon nanotube/polyhedral oligomeric silsesquioxane nanohybrid by utilizing click chemistry. *Nanoscale Res Lett.* 2011; 6:122.10.1186/1556-276X-6-122 [PubMed: 21711620]

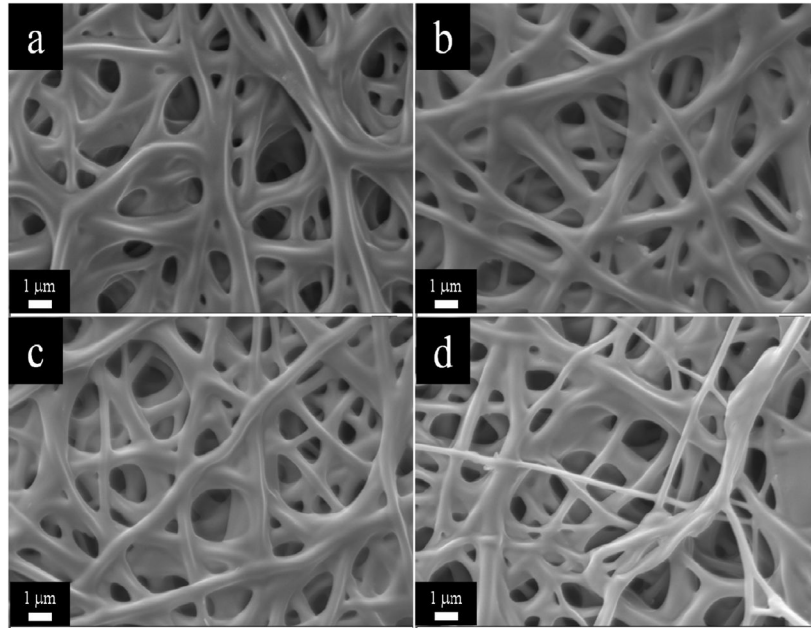


**Figure 1.** SEM images for the nanofibers that contain different amounts of MWCNTs: (a) 0%, (b) 0.06%, (c) 0.33% and (d) 0.66% of MWCNTs incorporated.

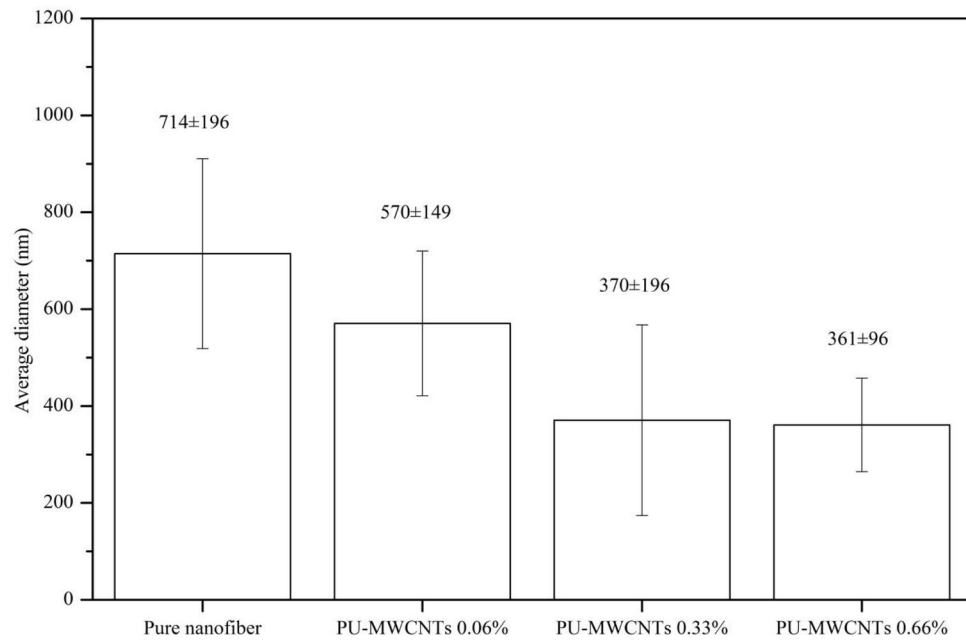


**Figure 2.**  
The average diameters of obtained nanofibers.



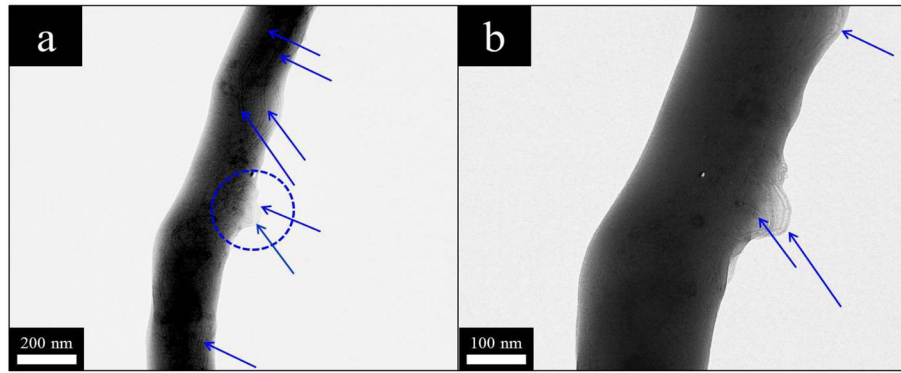


**Figure 3.** TEM micrograph of the nanofibers with MWCNTs, arrows indicating the location of MWCNTs (a). The high resolution images of the encircled area of former figure, indicating de-bundling of MWCNTs.

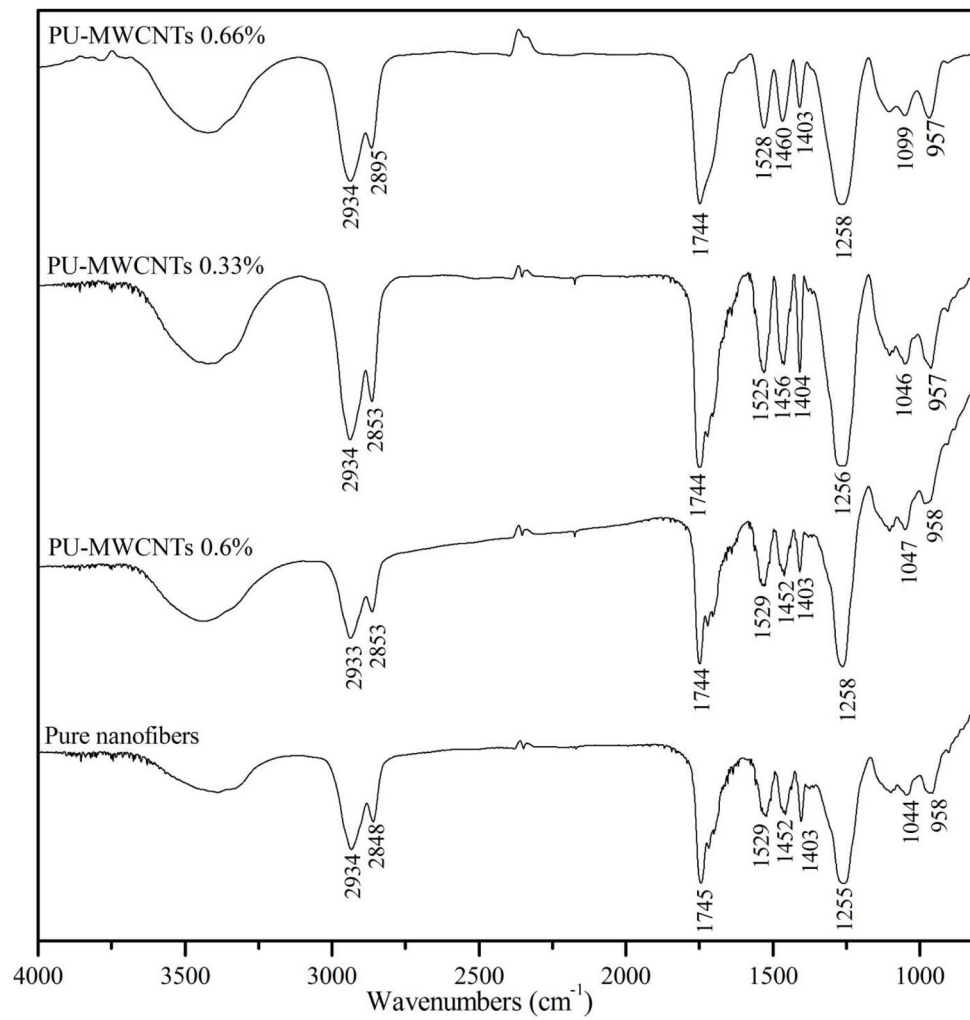


**Figure 4.**  
The FT-IR spectra of the pristine nanofibers mats and nanofibers incorporated with MWCNTs.

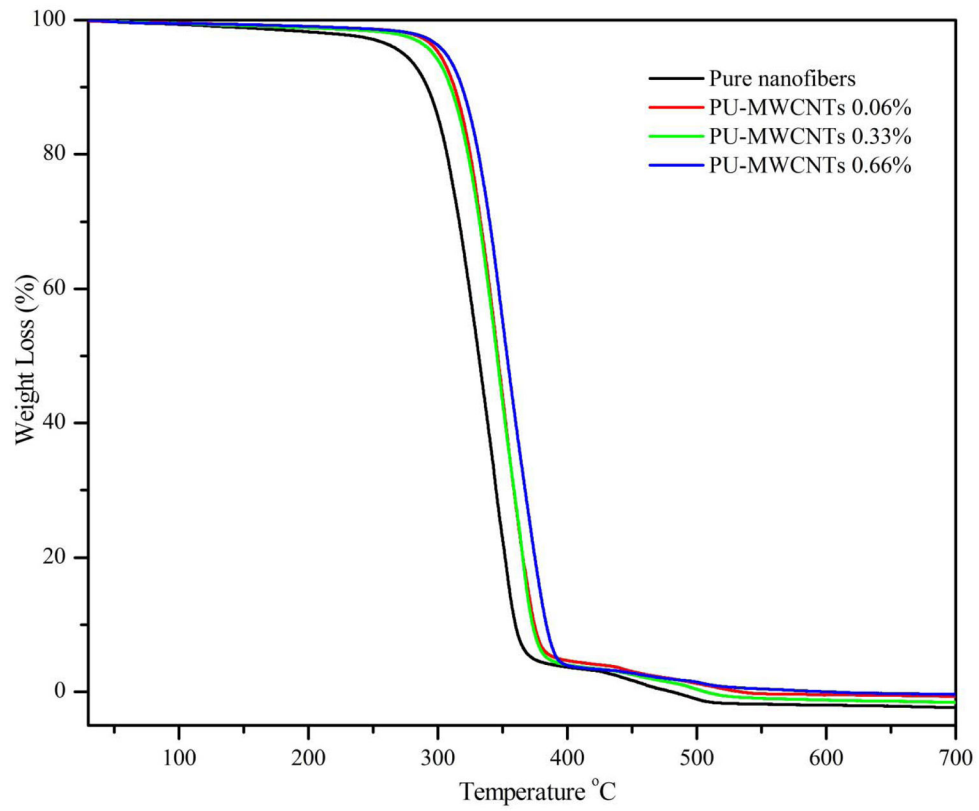


**Figure 5.** The thermogravimetric analyses of the pristine nanofibers and the nanofibers incorporated with MWCNTs.

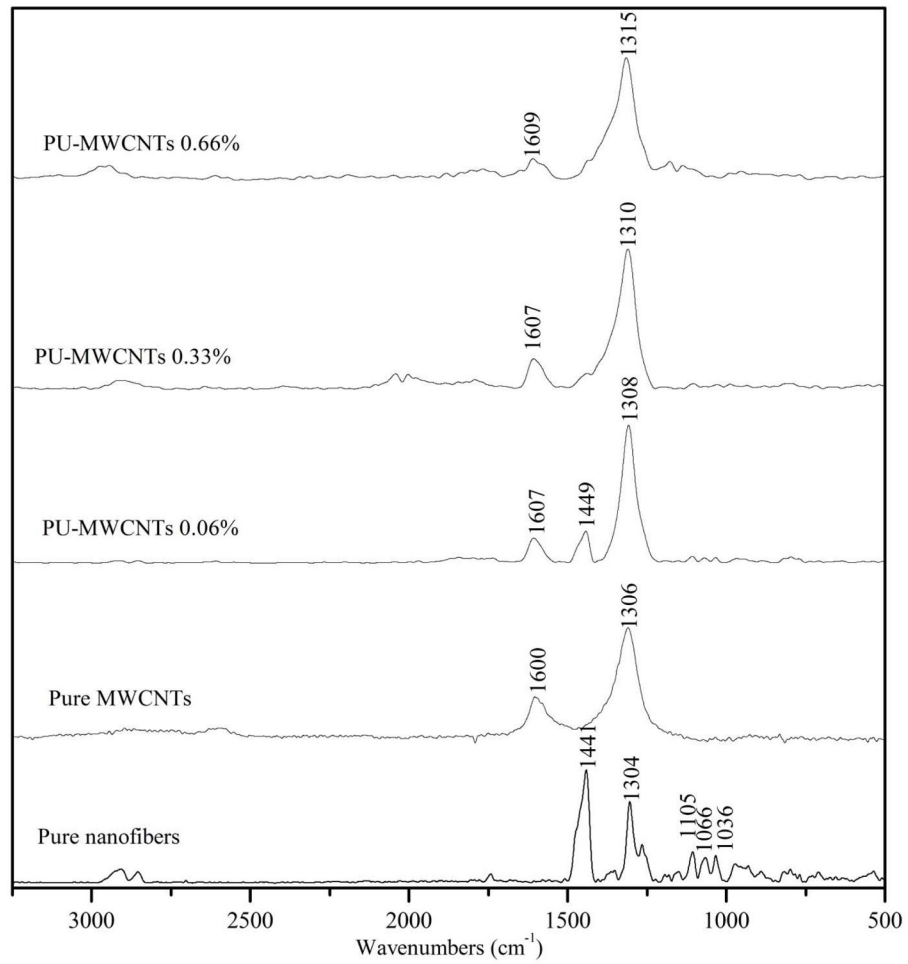


**Figure 6.** The Raman spectra of the pristine nanofibers, pure MWCNTs and the nanofibers with different concentrations of MWCNTs.

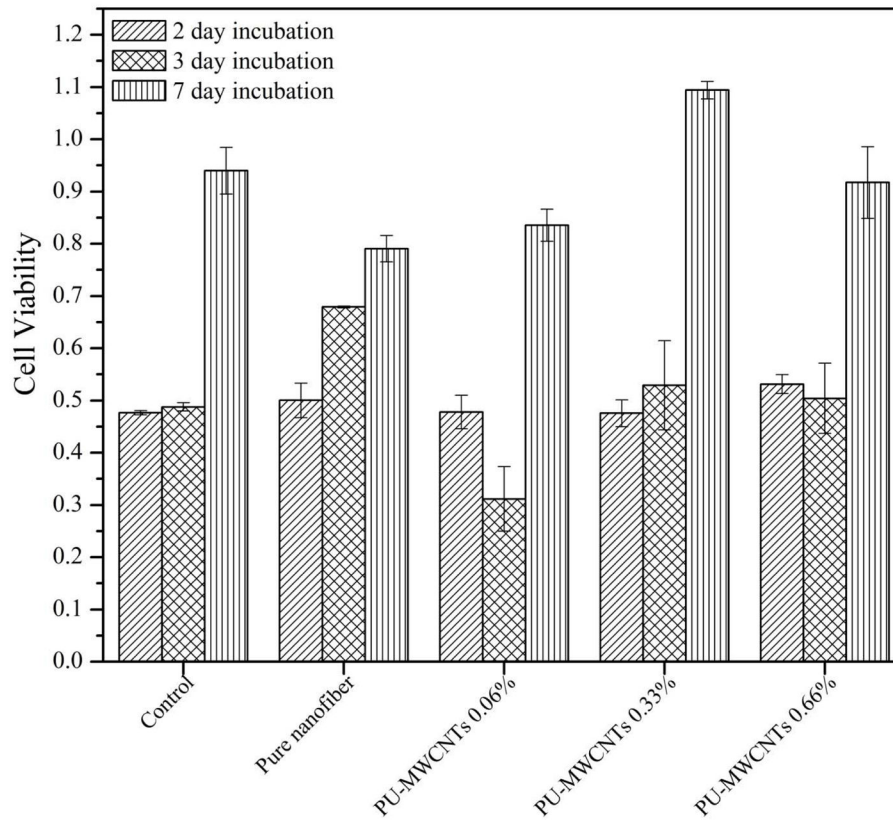


**Figure 7.**  
Results from the MTT assay for the pristine and the nanofibers with MWCNTs.

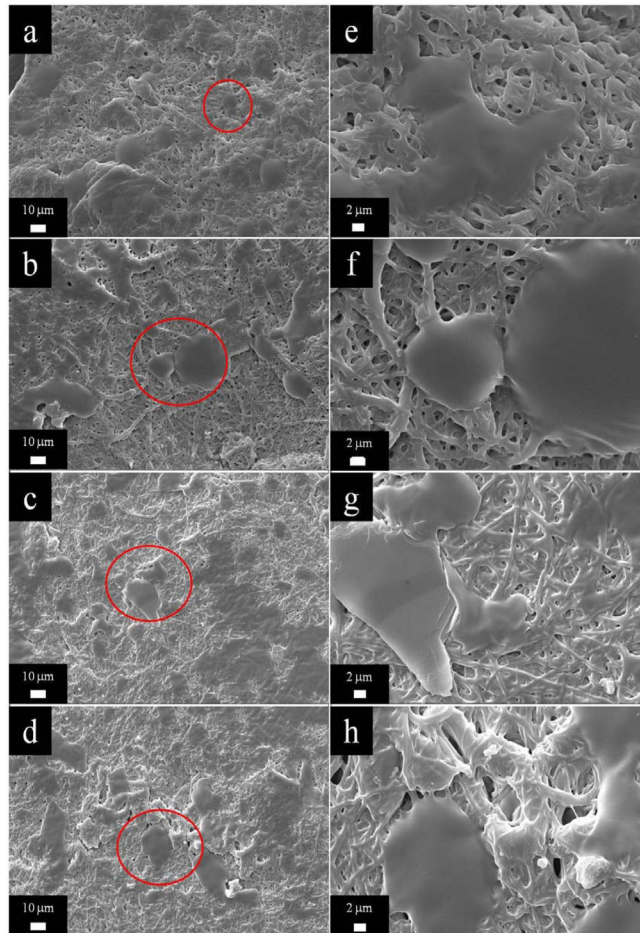


**Figure 8.** SEM images after culturing the NIH 3T3 fibroblasts in presence of nanofibers, after the 7 day of culture. Nanofibers containing different amounts of MWCNTs: (a) 0%, (b) 0.06%, (c) 0.33% and (d) 0.66% of MWCNTs in low magnifications. And, the nanofibers with different amounts of MWCNTs (e) 0%, (f) 0.06%, (g) 0.33% and (h) 0.66% of MWCNTs in high magnification from the encircled areas from the low magnification images.

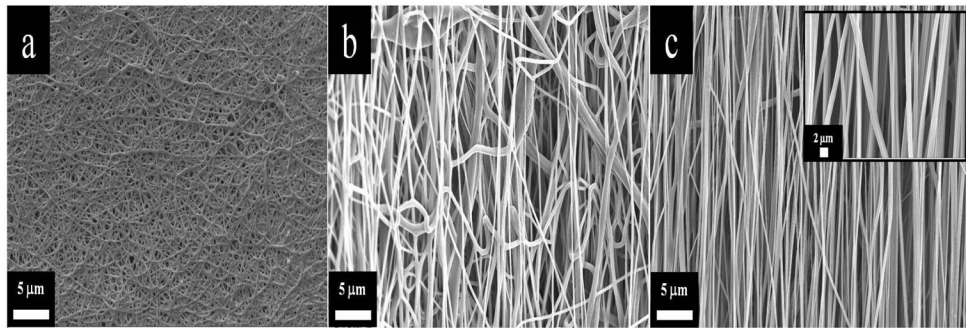


**Figure 9.** SEM images for the nanofibers containing 0.33% of MWCNTs, obtained upon increasing the rotation speeds of collecting drum: (a) Random, (b) Semi-aligned, (c) Completely aligned nanofibers.